Development of Radiation-Hard Solid-State Amplifiers for Kilogray Environments Using COTS Components

Chihiro Ohmori and Mauro Paoluzzi

***Abstract*— The high-luminosity Large Hadron Collider (LHC) (HL-LHC) project is the upgrade of the LHC to increase its luminosity by a factor of 5 compared with the nominal value. The LHC injector upgrade (LIU) project aims at upgrading the LHC injector chain to reach the goal of the HL-LHC. The LIU project covers all injectors, that is, the Linac 4, proton synchrotron (PS) booster (PSB), PS, and super PS (SPS). In the PSB, the present ferrite-loaded RF accelerating systems will be replaced with magnetic alloy (Finemet)-loaded cavity systems. The cavity system allows the implementation of a cellular topology and the use of solid-state RF power amplifiers. The PSB will have 144 cavity cells and amplifiers, and each amplifier uses 17 high-power MOSFETs. The RF systems will be installed in the straight sections where the total ionization dose (TID) is 20 Gy(Si)/year, which may even increase after the upgrade. Research and development work has been performed to validate the use of solid-state amplifiers in this radioactive environment. In this article, we describe a technique to stabilize the solid-state amplifier up to the total dose of about 10 kGy. This technique will enable the use of solid-state amplifiers in even higher radiation environments. The higher sensitivity to the single-event effects (SEEs) of the laterally diffused metal-oxide semiconductors (LDMOS) than to that of the vertical metal–oxide–semiconductor (VMOS) devices is also reported.**

***Index Terms*— Commercially off the shelf (COTS), MOSFET, proton synchrotron (PS), single-event effect (SEE), solid-state amplifier, total ionization dose (TID), wideband RF acceleration system.**

I. Introduction

THE Large Hadron Collider (LHC) injector upgrade (LIU) project [1], [2] includes the upgradation and consolidation of an RF system of the LHC injector chain to get ready for high-luminosity (HL)-LHC [3]. The present proton synchrotron (PS) booster (PSB) RF system consists of three different systems to cover the bandwidths for beam acceleration on $h = 1$, and the second-harmonic RF and higher harmonic RF for controlled longitudinal emittance blowup [4]. These systems occupy four straight sections in the booster. The magnetic alloy-loaded system [5] using Finemet [6], [7] will be installed in the straight sections, and its large instantaneous bandwidth (0.5–20 MHz) covers the frequency band of all the required harmonics [8], [9]. As the PSB consists of four superimposed accelerator rings, the RF system is made of four stacked systems assemblies. Each consists of a 12-cell cavity and corresponding solid-state amplifiers. In total, 48 cells are installed in a straight section and three straight sections are used for the whole RF system. Owing to this replacement, one straight section will be freed. The radiation levels in these straight sections are about 20 Gy(Si)/year. So far, solid-state amplifiers using a 300-W MOSFET have been employed in the prototype Finemet RF system, with the amplifiers directly connected to the accelerating gap and sit near the RF cavity.

LIU also includes a substantial increase of the PS beam intensity to be injected into the SPS. In the PS, longitudinal coupled bunch instabilities are observed [10] and could be damped by means of a spare RF cavity up to the beam intensity of 1.3×10^{11}ppb. A wideband longitudinal RF damper [11] has been installed in the PS to go above this intensity and damp simultaneously many different coupled bunch modes [12]. So far, 2.6×10^{11}ppb have been injected into the SPS as required by the project baseline. Here again, to drive the wideband magnetic alloy RF system, solid-state amplifiers are used in a configuration that is similar to that adopted in the PSB. Since the radiation dose in the chosen PS area is about 1 kGy(Si)/year [13], the solid-state amplifiers are installed under the wideband RF cavity with an iron shielding.

Further reduction in the equivalent impedance presented by the RF cavities to the circulating beams can be achieved by increasing the gain of the fast feedback loop in the PS RF systems, as in the 10-MHz cavities [14]. The goal is to mitigate the beam loading effects of the high-intensity beams. So far, tube amplifiers have been used in the fast feedback chain because of the high radiation level [15], reaching the limit allowed by this technology [14]. A further increase in the feedback gain could be envisaged only by employing a solid-state amplification stage. Increased gain requires small group delay, which is possible only with the feedback amplifier near the cavity, where extra shielding can hardly be added to protect the amplifier from radiation damage. A radiation-hard solid-state amplifier fitting the high radiation environment of the PS tunnel would, therefore, be mandatory.

CERN and KEK/J-PARC have been cooperating to develop the wideband Finemet-based RF systems for the PSB and

Manuscript received July 10, 2019; revised July 30, 2019 and August 20, 2019; accepted August 21, 2019. Date of publication August 26, 2019; date of current version October 21, 2019. This work was supported in part by Japan Society for the Promotion of Science (JSPS) KAKENHI under Grant JP18K11930 and in part by the Facility Service System of National Institutes for Quantum and Radiological Science and Technology (QST)-Takasaki.

C. Ohmori is with the J-PARC Center and KEK, Tokai 319-1195, Japan (e-mail: chihiro.ohmori@kek.jp).

M. Paoluzzi is with CERN, 1211 Geneva, Switzerland (e-mail: mauro.paoluzzi@cern.ch).

Color versions of one or more of the figures in this article are available online at http://ieeexplore.ieee.org.

Digital Object Identifier 10.1109/TNS.2019.2937603

TABLE I
LIST OF MOSFETS

type	geometry	manufacture	V_{DSS}
MRF151	VMOS	M/A com	125 V
SD2942	VMOS	ST Microelectronics	130 V
MRF151	VMOS	Motorola	discontinued
VRF151	VMOS	Microsemi	170 V
MRFE6VP6300	LDMOS	Freescale	130 V

the PS since 2012. The collaboration also included the test and development of radiation-hard, solid-state amplifiers using commercial off-the-shelf (COTS) components. Tests were carried out in radiation environments of the three institutes as well as in other irradiation facilities. In this article, we describe the strategy followed to choose MOSFETs for the PSB RF system and the developments performed to improve the radiation hardness of our devices. We also report recent developments of the radiation-hard solid-state amplifier for the high radiation environment of 8.8 kGy.

II. DEVELOPMENTS OF RAD-HARD SOLID-STATE AMPLIFIERS FOR THE PSB

A. Choice of MOSFET

In 2013, when the CERN accelerators were stopped during the first long shutdown, LS1, the first irradiation test of several power MOSFETs was carried out in the J-PARC main ring (MR), as listed in Table I. The MOSFETs of 300-W class were mounted on the printed circuit board (PCB) and installed at the downstream of the collimator. In the J-PARC MR, the beam loss is localized at the collimator position. Although the collimator is surrounded by an iron shielding, the scattered particles escape through the beam pipe and hit the MOSFETs on the PCB. The radiation dose was measured by the RadMon system developed at CERN [16]. Because the MR is a PS, the test area is a mixed field of radiations including gammas, charged particles, and neutrons. The rate of TID was 500 Gy(Si)/day after adjusting the collimator. The particle energy flux spectrum was estimated by the simulation code, particle and heavy-ion transport code system (PHITS) [17], [18]. It shows that protons and pions are the main fraction of the high-energy (>10 MeV) charged particles, and neutrons and photons distribute in a wide range of energies. The RadMon worked up to 4.2 kGy(Si). As shown in Fig. 1, the TID is proportional to the number of protons. After the RadMon stopped working, the total dose was estimated from the total number of protons. During the test, a 15-kW beam was delivered to the slow extraction during 10 days, followed by a 200-kW beam delivered to the T2K experiment. In total, a TID of 12 kGy(Si) and an integrated neutron flux of 7.2×10^{13} n/cm^2 (1 MeV-equivalent) were provided during the irradiation. The ratio between the TID and the neutron flux was 0.60×10^{13} n/cm/kGy(Si) at the J-PARC MR. The irradiation test also aimed at assessing the risk related to SEEs, on the high-power MOSFETs in view of their use in hadron accelerators. In the PSB, vertical metal–oxide–semiconductor (VMOS)-type MOSFETs have been used for decades in the feedback amplifiers of the final stage of the RF

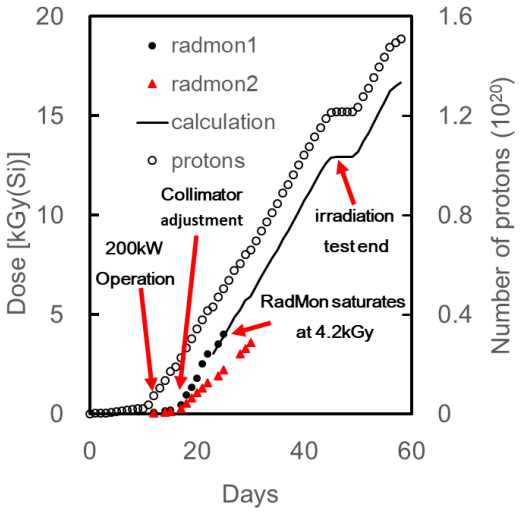

Fig. 1. TID and number of protons during the MOSFET test at the J-PARC. RadMon #1, which is on the MOSFETs, is used as a reference of the dose that MOSFETs received. Expected dose was calculated from total protons.

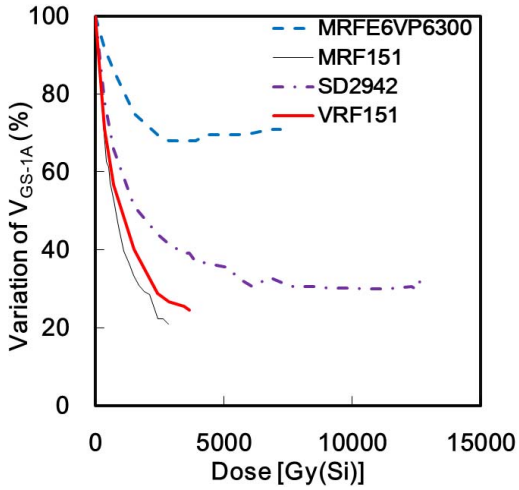

Fig. 2. Results of the irradiation test of MOSFETs at the J-PARC MR in 2013. The radiation effects on four different MOSFETs are shown as variations in the gate threshold voltages for the drain current of 1 A.

acceleration systems. The possibility of single-event burnout (SEB) and single-event gate rupture (SEGR) was pointed out for the use of high-power MOSFETs [19], [20], and their destructive effects were indeed observed. For their evaluation, the MOSFETs were placed in parallel to the beam to mimic the amplifiers in the PSB tunnel.

The control system of the devices was located in the power supply building, which is about 200 m away from the setup. A drain voltage of 48 V was applied for each MOSFET. The gate voltage of each MOSFET was ramped from 0 to 10 V in 1 ms to measure the drain current. The drain currents were measured every hour. Before the measurements, the control system checked the status of each MOSFET. Fig. 2 shows the results of the irradiation test. The radiation effects on the MOSFET appeared as the drifts of the gate bias voltage. Fig. 2 shows the variations in the bias voltage for the drain current of 1 A. The vertical-style MOSFETs, VMOS, show a larger

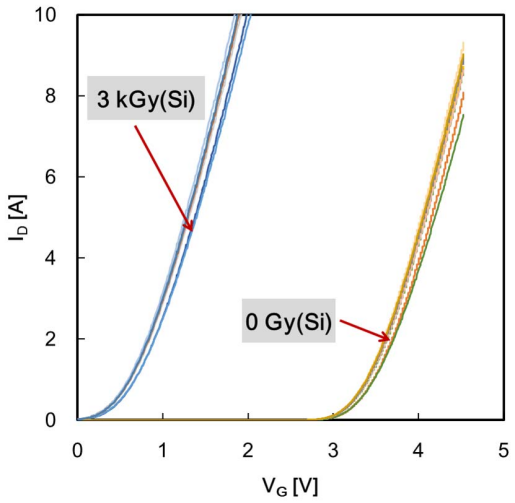

Fig. 3. Irradiation test of MOSFETs, VRF151, at the Fraunhofer Institute. In the test, eight MOSFETs were tested and all show the same behavior before and after 3-kGy(Si) irradiation.

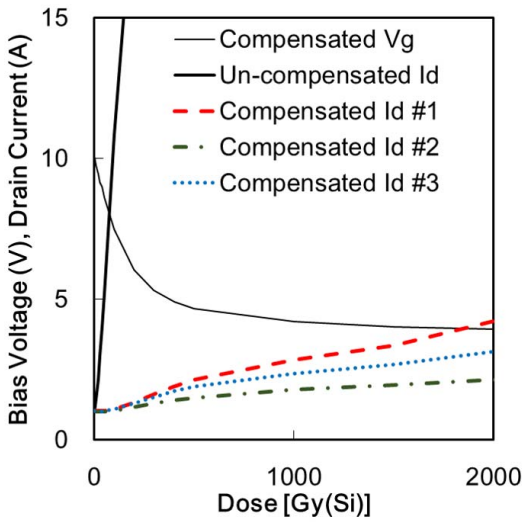

Fig. 4. Mitigation test of MOSFETs, VRF151, at the Fraunhofer. It shows that the drain currents were stabilized by applying the compensated bias voltage on the gate of each MOSFET.

variation, while laterally diffused metal-oxide semiconductors (LDMOS) show less variation. All MOSFETs survived a dose in excess of 2 kGy(Si), which corresponds to many years of operation in the PSB. No failures caused by SEE were measured up to 2 kGy(Si). As shown in Table I, these MOSFETs have different drain–source breakdown voltage.

The solid-state amplifiers in the PSB will drive the cavity directly and large voltages are expected to be induced by the circulating beam. The MOSFET VRF151, a vertical double-diffused MOS, VDMOS type, which has the largest V_{DSS}, was selected for the final-stage amplifiers in the PSB. The large V_{DSS} also ensures a large-voltage derating, which is known to limit the device's sensitivity to the SEE [21].

B. Mitigation of Radiation

After the irradiation test at J-PARC, the test was continued at the Fraunhofer Institute using the gamma rays of ^{60}Co. For this, another setup with the new MOSFETs was produced. Fig. 3 shows the behavior and variation of bias characteristics of eight MOSFETs of type VRF151. All of them show the same behavior before and after the irradiation of 3 kGy(Si). The gate threshold voltage for the drain current of 1 A drops to 20% of the initial value, consistent with the results obtained at J-PARC (Fig. 2). It is the TID effect on the power MOSFET. Although the TID effects are less problematic in digital and high-performance analog CMOS technologies, because SiO_2 gate dielectric layers are thin, power MOSFETs still need thickness to withstand high drain–source voltage, V_{DSS} [22]–[24].

As the radiation effects seem reproducible, a mitigation test was carried out. It used a sensing device to generate a reference gate voltage proportional to its threshold voltage, V_{TH}. The reference voltage was then applied to all amplifier devices, thus collectively compensating changes due to radiations. Three MOSFETs were tested using a sensing device. The results are shown in Fig. 4. A MOSFET without mitigation shows rapid variation in bias characteristics. As the drain current increases rapidly, the power dissipation will become unacceptable. The other three MOSFETs with the mitigation show stable behaviors and survived up to 2 kGy(Si).

C. Radiation Environments in the PSB

The radiation level in the straight sections available for the installation of the RF systems in the PSB tunnel was measured using the RadMon system. The highest radiation dose, found in section 10L1, is about 20 Gy(Si)/year. It may become slightly larger after full implementation of LIU. This value is two to five times higher than in the other available sections and corresponds to a sufficiently long lifetime of the VRF151 MOSFET (many years of operation).

D. Power Test Under the Radiation

It is known that the radiation effects on MOSFETs also depend on the temperature and operation conditions. We prepared a setup to test solid-state amplifiers under the gamma-ray irradiation. During the irradiation test, the amplifier generated 100 W of RF power sweeping the frequency from 0.5 to 5 MHz. MOSFET #1, used in the amplifier, was mounted on an aluminum heat sink and was cooled by a cooling fan. Next to the amplifier, MOSFET #2 was mounted on another cooling unit to monitor the radiation effect. The gate voltage was adjusted to allow a constant current flow to the MOSFET #2 and the same gate voltage was supplied to MOSFET #1 in the amplifier to mitigate the radiation effects. An automatic level control (ALC) loop was used to stabilize the RF output to 100 W. A dummy load was mounted behind MOSFET #2 and was cooled by the fin fan cooler. The RF power was monitored and the monitor signal was sent to the ALC circuit. The circuit diagram of the system is shown in Fig. 5.

We prepared two amplifier's setups. They were located at 15 and 2 Gy/h. The dose was measured using an Aminogray, Alanine dosimeter [25], [26]. The amplifiers were irradiated

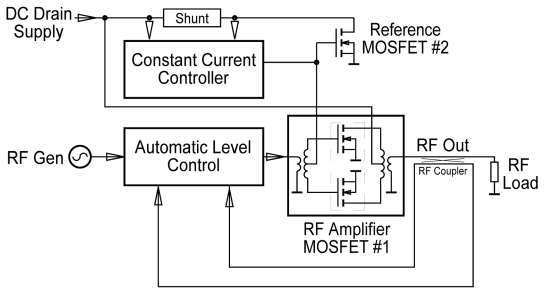

Fig. 5. Circuit diagram of the 120-W amplifier with the mitigation circuit.

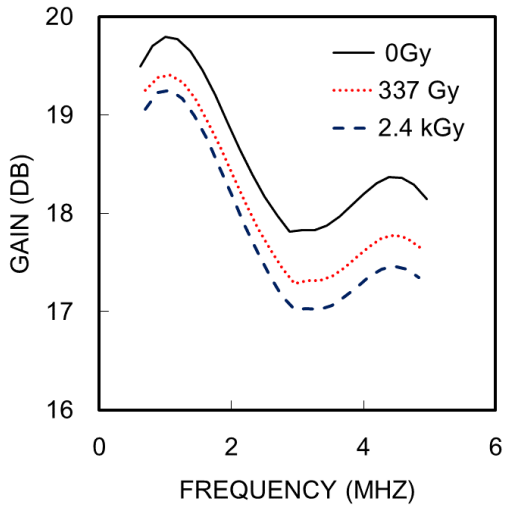

Fig. 6. Variations in the amplifier gain and gate bias voltages by the gamma-ray radiation. The amplifier was irradiated with the dose rate of 15 Gy/h for 160 h.

for 160 h in total, resulting in accumulated doses of 2.4 kGy and 320 Gy, respectively. Both the amplifiers were driven during the irradiation test with 100% duty factor. The RF frequency was swept with a 2-min cycle. The RF amplitudes of the input and the output were rectified and recorded using a data logger. The RF phases of the RF outputs were detected by the phase detector. The gate voltage to mitigate the radiation effects for both the amplifiers showed the same behavior of the radiation.

The results of the radiation test are shown in Fig. 6. Both the setups survived and variations in the amplifier gain between 0.5 and 5 MHz were about 1 dB. Fig. 7 shows the gain variation at 0.5 MHz and the gate bias to stabilize the drain current to 1 A. Figs. 6 and 7 show that the gain variation occurs at the beginning of the irradiation below 300 Gy. When using solid-state amplifiers to drive the RF cavities, a gain variation of about 1 dB is acceptable, because an ALC loop is usually used to stabilize the RF voltage. Although gain variations were observed, a variation in phase was not observed during the test. The results can be explained by the behavior of the transconductance in Fig. 3. It shows that the characteristics of the MOSFET were shifted to a lower gate voltage without changing the shape by the radiation effects. If the shape is the same, the transconductance, g_{mn}, will be the same when the

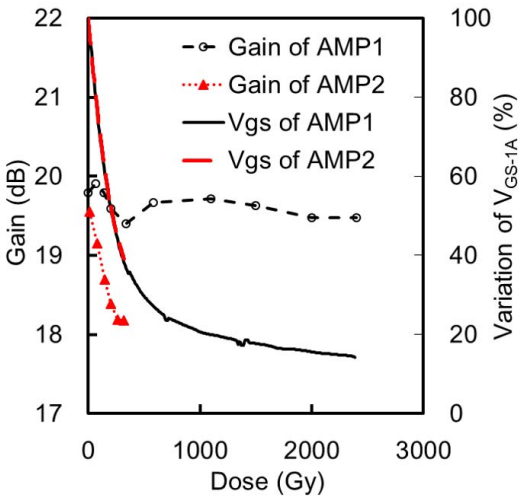

Fig. 7. Variations in the amplifier gains at 0.5 MHz by the gamma-ray irradiation. The gain variations occurred at lower dose.

same idling current was supplied by adjusting the gate voltage, properly.

E. Mixed-Field Radiation Test at the CHARM Facility

Following the tests at QST-Takasaki, the solid-state amplifier was shipped to CERN and the MOSFETs were replaced for testing at the CERN High-energy AcceleRator Mixed-field facility (CHARM) [27], [28]. CHARM uses the proton beam of the PS. Particles scattered from a Cu target, including gamma rays, charged particles, neutrons, and other hadrons, will hit the components under test. Total ionization dose (TID) and neutrons are measured by the RadMon, which was placed near the amplifiers [29]. Another amplifier using LDMOS was also tested, as described in Section III-B. To obtain high TID, both amplifiers were located in longitudinal position [27] near the beamline. The scattered high-energy hadron particles hit the amplifiers from the front, perpendicularly. The other mixed-field radiations to the amplifiers were quasi-isotropic. The irradiation test was carried out for three weeks and a total number of 5.25×10^{16} protons were delivered.

Fig. 8 shows the results under the mixed-field radiation at CHARM [30]. The amplifier using VRF151 survived until the end of the experiment. A total dose of 1.9 kGy(Si) and a neutron flux of 1.1×10^{13} n/cm were delivered. The variation in the gain due to the radiation was about 1 dB, as shown in Fig. 8, and it is consistent with the result at QST-Takasaki shown in Fig. 7. The behavior of gate bias was also similar. It shows that the gain variation occurred below 300 Gy(Si). It is also consistent with the gamma-ray irradiation, as shown in Fig. 7. These results suggest that the variation in the amplifier gain using VRF151 is dominated by the total dose-effect and it does not depend on the flux of neutrons and other particles.

At CHARM, the ratio of the TID and neutron flux is 0.57×10^{13} n/cm^2/kGy(Si). It is interesting that the ratio is almost the same as the number of the J-PARC MR collimator section (0.60×10^{13} n/cm^2/kGy(Si)) although the beam loss at the

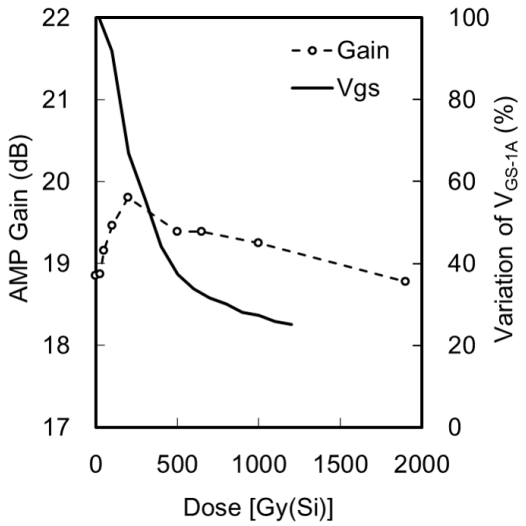

Fig. 8. Gain variation at 0.5 MHz under the mixed field radiation at the CHARM.

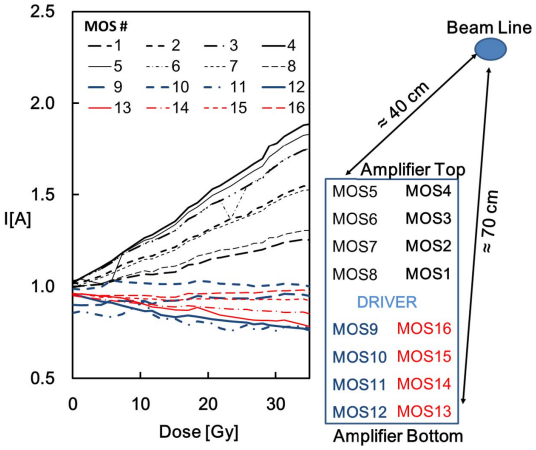

Fig. 9. Effect of position. A 3-kW solid-state amplifier was set below the damper cavity without any radiation shielding. The drain current of each MOSFET was measured showing position dependence.

J-PARC occurred around 3 GeV and CHARM uses a 27-GeV proton beam.

F. Effect of the Position With Respect to Beamline and Reference MOSFET

A 3-kW-solid-state amplifier was installed in the CERN PS to observe the effect of different MOSFET positions with respect to the beamline and the reference MOSFET on compensation. An amplifier was placed right under the PS damper without any radiation shielding. It used 18 MOSFETs, including one as the driver and another as the reference for the compensation. The driver and radiation reference MOSFETs were placed in the center of the amplifier. The 16 other devices were placed in couples vertically above and below, as shown in Fig. 9, which also indicates the beamline position. It also shows the variation in the drain current of the 16 MOSFETs during the deposition of the first 50 Gy(Si). It can be seen that the devices closer to the beamline than the reference MOSFET were undercompensated, while the compensation of those on the same level or below was reasonably good. This can be explained by a higher dose deposition on the closer devices. This assumption was verified by turning the amplifier upside down, thus inversing the device distance from the beamline. The result of the irradiation test showed that, as expected, the current variation rates inverted with the amplifier mounted upside down. The reference MOSFET for the compensation was located beside the driver MOSFET. It clearly shows that the MOSFETs in the upper side of the amplifier had a large drift because the compensation was not enough. The other MOSFET in the lower side shows overcompensation. It can be explained by the upper half receiving more dose than the reference MOSFET while the lower set received fewer doses.

G. Evaluations for the Usages

In the PSB, the dose rate is much smaller than that in the PS, and it is expected that the effect of the MOSFET position will occur slowly. Fig. 9 suggests, however, that the compensation scheme using one reference MOSFET is not perfect. Fortunately, synchrotrons typically have an RF-off period, when the beam is extracted and the magnets ramp down. Another scheme using the idling currents of all MOSFETs to adjust each gate voltage during this RF-off period can thus be envisaged.

The irradiation tests using ^{60}Co and mixed field show that the solid-state amplifier using VRF151 survives up to 2 kGy. So far, no failure was observed, neither SEE nor otherwise. The dose of 2 kGy corresponds to about 100 years of operation in today's PSB.

Moreover, the solid-state amplifiers for the PS damper system, which are protected by the iron shielding, will receive 50 times less dose than the outside of the shielding, as shown in Fig. 10. It can thus be expected that the solid-state amplifiers for the damper system also have an acceptable lifetime.

III. Developments of Rad-Hard Solid-State Amplifiers for the PS Environment of 1 kGy/Year

A. Radiation Test of VMOS for 10-kGy Environments

The solid-state amplifiers using vertical-type VDMOS, VRF151, satisfy the requirements for use in the PSB tunnel. With iron shielding, it is also possible to use them in the PS ring. However, tests at higher dose are required to qualify them for use in the PS ring without shielding. The feedback amplifiers in the final stage under the 10 MHz cavities require the robustness for the high radiation dose of several kilograys.

Another irradiation test using ^{60}Co was carried out at QST-Takasaki. Fig. 11 shows the variation in the amplifier gain exposed to 8830 Gy, measured by the Aminogray. The MOSFET, VRF151, shows the variation in the gain of about 1 dB. It is about the same as that in the irradiation tests at QST-Takasaki and CHARM, as shown in Figs. 7 and 8. The results suggest that solid-state amplifiers can be used for the feedback chain of the 10-MHz RF systems. The use of the solid-state amplifiers will improve the feedback gain [14].

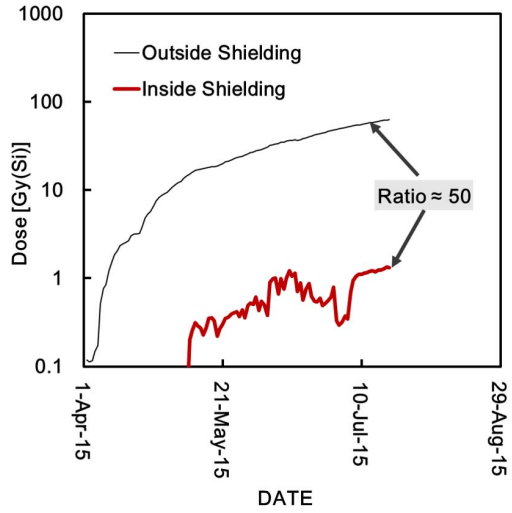

Fig. 10. Dose inside and outside of the iron shielding.

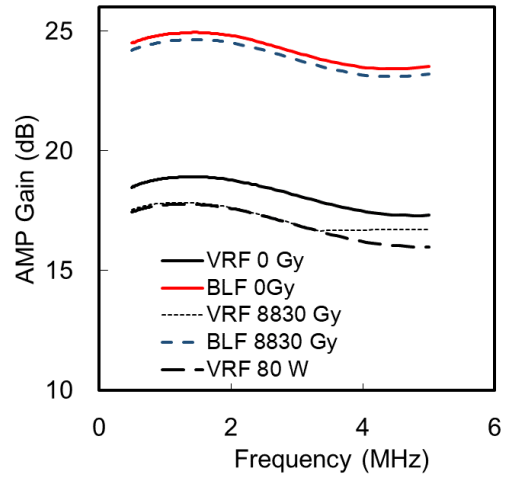

Fig. 11. Variation in the gain after exposure to 8830 Gy by the gamma-ray irradiation. Because of the shortage of RF input of the 120-W amplifier, the gain at the frequency higher than 3.5 MHz was not measured properly. The gain was also measured with the output power of 80 W.

B. Radiation Test of LDMOS

The LDMOS is also used for RF power amplifiers. The radiation test at the J-PARC MR suggests that the LDMOS might be less sensitive to the radiation, as shown in Fig. 2. Although the V_{DSS} is low, as listed in Table II, the use of the feedback may still be possible as it is not affected by the beam directly.

A 500-W-class LDMOS was assembled in a push–pull, class AB amplifier and tested at QST-Takasaki. In the test, the compensation scheme adopting the circuit, as shown in Fig. 5, was used. To improve the compensation, the MOSFETs for reference and the amplifier were located close together. The results are also shown in Fig. 11. The amplifier using the LDMOS worked well until the end, and the gain variation is much less than that in the VMOS amplifier.

The LDMOS amplifier was also tested at CHARM in 2017 and exposed to a total dose of 1.9 kGy(Si). The results

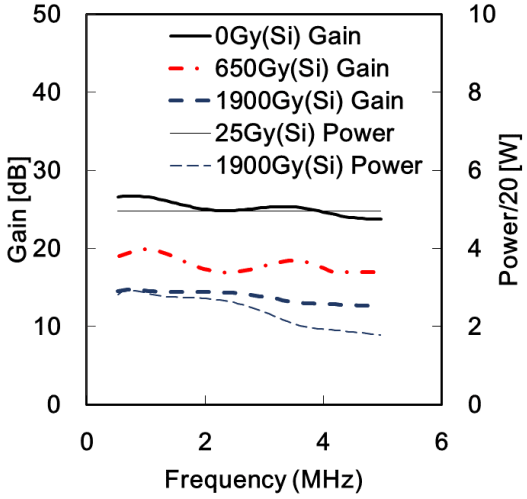

Fig. 12. Variations in the amplifier gain and output power by 1.9-kGy(Si) irradiation at CHARM. The output power also reduced to 40 W by the mixed-field irradiation.

are shown in Fig. 12. The gain drop started already below 650 Gy(Si) and a failure occurred. The behaviors were very different from the VDMOS, as shown in Fig. 8. SEE is suspected as the cause of the failure.

The test of the LDMOS was repeated at CHARM in 2018. In total, a TID of 1150 Gy(Si) and a neutron flux of 9.3×10^{12} n/cm^2 were irradiated on the sample. The amplifier was mounted on a heat sink for cooling. It was operated at a 100-W fixed output power in the pulsed mode. The frequency was swept from 0.5 to 5 MHz. The pulselength was 9.5 s and the repetition time was 10 s for the first 170 h and then 20 s. A compact controller, which is developed for the PSB, was used. It is used to adjust the gate bias to the constant drain current when the RF is off. The scheme is shown in Fig. 13. The quiescent current was set to 1 A total (0.5 A per MOSFET). The results plotted in Fig. 14 show that the gate bias, starting from 1.7 V, initially lowered as the TID builds up. After about 90 h (320 Gy(Si)), a sudden quiescent current drop was recovered by the controller that increased the gate bias to 4 V following a failure caused by the SEE.

Measurement of the MOSFET characteristics at the end of the test showed that the gate–source resistance dropped to a few tens of ohms. With this low value, the controller, designed to work on kiloohm loads, could not maintain the correct bias condition. The resistance change happened in steps as shown by the gate-voltage-stepped changes (Fig. 14), suggesting the occurrence of the SEE. Using the RF drive, the device's transconductance was measured (Fig. 15) and it is showing a threshold displacement as well as a 35%–45% reduction. Comparing with Fig. 3, the variation in the transconductance may explain the gain reduction of the LDMOS amplifier.

Another test on the LDMOS was also carried out at Paul Scherrer Institute (PSI) supporting the conclusion that the cause of the failures in the mixed radiation field was the SEE [31]. It is thus understandable that the variation in transconductance could not be compensated by shifting the gate voltage.

TABLE II
PARAMETERS OF MOSFETS

type	geometry	manufacture	V_{DSS}	Output	Typ. Gain	applications
VRF151	VDMOS	Microsemi	170 V	300 W	18 dB	Final Stage AMP
BLF574	LDMOS	NXP	110 V	500 W	24 dB	feedback AMP

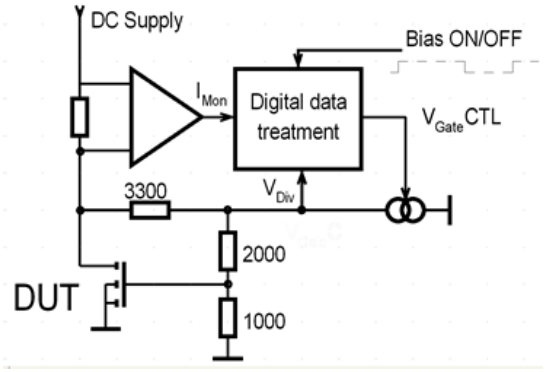

Fig. 13. Schematics for the constant drain rest current to mitigate the radiation effects. Beamoff timing is used to measure the rest of the current and to adjust the gate voltage of the MOSFET.

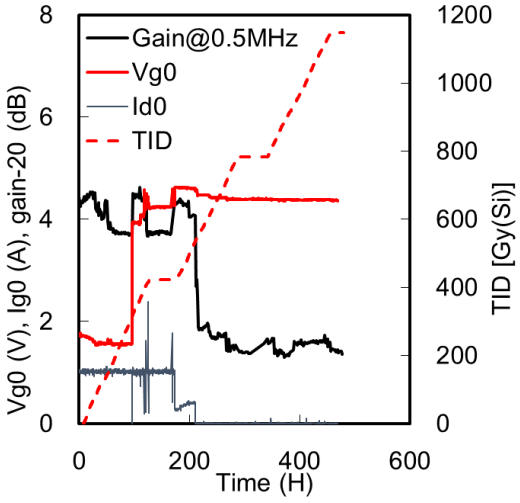

Fig. 14. Variation in the amplifier gains, gate voltage, idling drain current, and TID. In total, TID of 1.1 kGy(Si) and 9.3×10^{12} n/cm^2 were irradiated on the amplifier using an LDMOS.

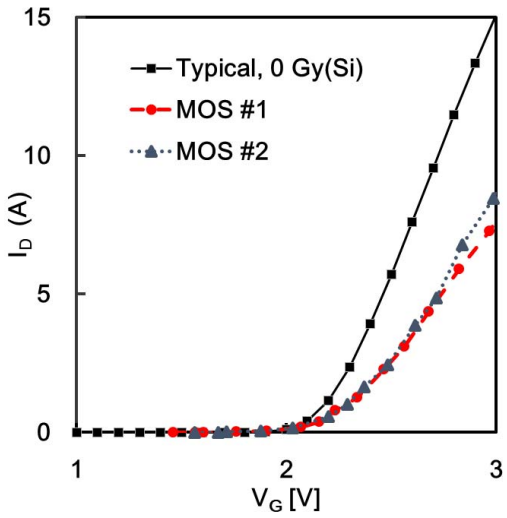

Fig. 15. Variation in device transconductance of an LDMOS before and after irradiation.

IV. DISCUSSION

A. Mitigation Schemes

In the case of RF power applications in radiation environments of PS, including gammas, charged particles, and neutrons, VMOS devices proved good hardness to SEE and high sensitivity to TID. The TID effects basically alter the gate threshold voltage and this effect can be mitigated using some kind of correction. In a first mitigation approach, one device was used to derive the required correction. However, for the special case of RF applications of particle accelerators, the idling currents of MOSFETs can be measured after beam extraction from the accelerator during RF-off. For example, the cycle time of the PSB is 1.2 s and it includes the magnet ramping down time and magnet off time. It is a common feature of synchrotrons to have a ramping down time during the cycle. During the period, no particle circulates in the machine and the RF system can be operated to compensate the radiation effects. Therefore, real-time compensation can be applied during the accelerator operation. This mitigation scheme is unique and different from those used in the space applications [32], which adopt the variation in pulsewidth for adjusting the gate voltage to mitigate the TID effects, as well as a low-noise amplifier [33] with a performance-tuning algorithm. In these cases, the radiation effects can be monitored as a variation in the pulsewidth. In accelerator RF systems, for stable beam acceleration, the RF frequency and pulsewidth cannot change; therefore, a dedicated measurement time to evaluate radiation effects is necessary.

The additional advantage of this technique is that it can be used for higher power amplifiers, which consist of many MOSFETs. Although each MOSFET receives a different dose, the simple multi-channel mitigation scheme shown in Fig. 13 will handle the compensation separately. In the PSB, 144 solid-state amplifiers will be installed and each amplifier has 17 MOSFETs. All MOSFETs will be mitigated independently.

B. Application to Medical Synchrotrons

In many proton and heavier ion synchrotrons for cancer treatments, magnetic alloy cavities are used [34], [35]. These cavities are driven by solid-state amplifiers located at a significant distance to protect them from radiation. However, there are reflection, impedance mismatch, and RF power-transfer efficiency problems when inserting long coaxial cables

between the cavity and the amplifier. The developments of radiation-hard solid-state amplifiers using mitigation schemes will solve this problem by allowing the location of the amplifier close to the cavities. The expected TID in medical accelerators is much lower than 10 kGy.

V. Conclusion

Rad-hard solid-state amplifiers using COTS components were developed for use in kilogray mixed-field environments. The mitigation scheme to compensate the TID effects works well for VDMOS-type MOSFETs up to a total dose of 8.8 kGy for gamma rays. Long lifetime is expected when using solid-state amplifiers for the CERN PSB RF system and the PS damper system. Research and development efforts have been continued to investigate the use of solid-state amplifiers for the RF feedback chain without radiation shielding. Another mixed-field irradiation test is planned for 2019.

Acknowledgment

The authors would like to thank S. Danzeca for identifying the cause of failure on the LDMOS. They would like to thank M. Shirakata, M. Yoshii, F. Tamura, K. Hasegawa, and J-PARC Ring RF Group for their supports for beam test; R. Gaillard, S. Gilardoni, M. Brugger, and G. Spieza, the CERN CHARM Support Group, and the CERN RF Group for helping us with beam tests; and S. Albright, E. Jensen, and C. Rossi for brushing up the article.

References

[1] M. Meddahi *et al.*, "LIU technical design report," CERN, Geneva, Switzerland, Tech. Rep. CERN-ACC-2014-0337, vol. I, 2015.
[2] J. Coupard *et al.*, Eds., "LIU technical design report," CERN, Geneva, Switzerland, Tech. Rep. CERN EDMS LIU-PM-RPT-00257, 2016, vol. 2.
[3] G. Arduini *et al.*, "Beam parameters at LHC injection," CERN, Geneva, Switzerland, Tech. Rep. CERN-ACC-2014-0006, 2014.
[4] D. Valuch, "Radio frequency systems of the CERN synchrotron accelerators," in *Proc. 19th Int. Conf. Radioelektronika*, Apr. 2009, pp. 17–24.
[5] C. Ohmori *et al.*, "Development of a high gradient rf system using a nanocrystalline soft magnetic alloy," *Phys. Rev. Accel. Beams*, vol. 16, no. 11, Nov. 2013, Art. no. 112002.
[6] Y. Yoshizawa and K. Yamauchi, "Common mode choke cores using the new Fe-based alloys composed of ultrafine grain structure," *J. Appl. Phys.*, vol. 10, no. 64, pp. 6047–6049, Mar. 1988. doi: 10.1063/1.342150.
[7] *Nanocrystalline Soft Magnetic Material, Finemet*. [Online]. Available: http://www.hitachi-metals.co.jp/products/elec/tel/pdf/hl-fm9-h.pdf
[8] M. Paoluzzi, "Design of the PBS wideband RF system," CERN, Geneva, Switzerland, Tech. Rep. CERN-ACC-NOTE-2013-0030, 2013.
[9] M. Paoluzzi *et al.*, "The new 1-18 MHz Wideband RF system for the CERN PS booster," in *Proc. 10th Int. Particle Accel. Conf.*, 2019, pp. 3063–3065.
[10] H. Damerau *et al.*, "Excitation of longitudinal coupled-bunch oscillations with the wide-band cavity in the CERN PS," in *Proc. 7th Int. Part. Accel. Conf.*, 2016, pp. 1724–1726.
[11] M. Paoluzzi *et al.*, "Design of the PS longitudinal damper," CERN, Geneva, Switzerland, Tech. Rep. CERN-ACC-NOTE-2013-0019, 2013.
[12] H. Damerau *et al.*, "Longitudinal coupled-bunch instability studies in the PS," in *Proc. CERN-Injector MD Days*, 2017, pp. 59–62.
[13] J. Saraiva *et al.*, "Radiation levels at CERN's injectors and their impact on electronic equipment," CERN, Geneva, Switzerland, Tech. Rep. CERN-ACC-2015-091, 2015.
[14] G. Favia, "Design report of a 1 kW power ampli'er for the PS RF 10 MHz system," CERN, Geneva, Switzerland, Tech. REp. CERN-ACC-NOTE-2018-0048, 2018.
[15] D. Grier, "The PS 10 MHz cavity and power amplifier," CERN, Geneva, Switzerland, Tech. Rep. PS/RF Note 2002-073, 2002.
[16] G. Spiezia *et al.*, "The LHC radiation monitoring system RadMon," in *Proc. PoS*, 2011, p. 24.
[17] T. Sato *et al.*, "Particle and heavy ion transport code system PHITS, version 2.52," *J. Nuclear Sci. Technol.*, vol. 50, no. 9, pp. 913–923, Sep. 2013.
[18] M. Shirakata, "Estimation and measurements of radiation dose distribution for the radiation test area in J-PARC main ring," in *Proc. 8th Int. Part. Accel. Conf.*, 2017, pp. 4689–4691.
[19] *Methods for the Calculation of Radiation Received and Its Effects, and a Policy for Design Margins*, document ECSS E-ST-10-12C, 2018.
[20] J. L. Titus, "An updated perspective of single event gate rupture and single event burnout in power MOSFETs," *IEEE Trans. Nucl. Sci.*, vol. 60, no. 3, pp. 1912–1928, Jun. 2013.
[21] J. L. Titus *et al.*, "Impact of oxide thickness on SEGR failure in vertical power MOSFETs; Development of a semi-empirical expression," *IEEE Trans. Nucl. Sci.*, vol. 42, no. 6, pp. 1928–1934, Dec. 1995.
[22] D. M. Fleetwood, "Evolution of total ionizing dose effects in MOS devices with moore's law scaling," *IEEE Trans. Nucl. Sci.*, vol. 65, no. 8, pp. 1465–1481, Aug. 2018.
[23] T. R. Oldham and F. B. McLean, "Total ionizing dose effects in MOS oxides and devices," *IEEE Trans. Nucl. Sci.*, vol. 50, no. 3, pp. 483–499, Jun. 2003, doi: 10.1109/TNS.2003.812927.
[24] J. R. Schwank, M. R. Shaneyfelt, D. M. Fleetwood, J. A. Felix, P. E. Dodd, P. Paillet, and V. Ferlet-Cavrois, "Radiation effects in MOS oxides," *IEEE Trans. Nucl. Sci.*, vol. 55, no. 4, pp. 1833–1853, Aug. 2008.
[25] D. F. Regulla and U. Deffner, "Dosimetry by ESR spectroscopy of alanine," *Int. J. Appl. Radiat. Isot.*, vol. 33, pp. 1101–1114, Nov. 1982.
[26] T. Kojima, R. Tanaka, Y. Morita, and T. Seguchi, "Alanine dosimeters using polymers as binders," *Int. J. Radiat. Appl. Instrum. A, Appl. Radiat. Isot.*, vol. 37, no. 6, pp. 517–520, 1986.
[27] J. Mekki, M. Brugger, R. G. Alia, A. Thornton, N. C. D. S. Mota, and S. Danzeca, "CHARM: A mixed field facility at CERN for radiation tests in ground, atmospheric, space and accelerator representative environments," *IEEE Trans. Nucl. Sci.*, vol. 63, no. 4, pp. 2106–2114, Aug. 2016.
[28] *The Charm Facility*. [Online]. Available: http://charm.web.cern.ch
[29] G. Spiezia *et al.*, "A new Radmon version for the LHC and is injection lines," *IEEE Trans. Nucl. Sci.*, vol. 61, no. 6, pp. 3424–3431, Aug. 2014.
[30] M. Paoluzzi *et al.*, "RF Amplifier using VRF151G and BLF 574 power RF Mosfets," CERN, Geneva, Switzerland, Tech. Rep., 2017.
[31] S. Danzeca, *Radiation Test Report at PSI*. document CERN-EDMS-2037116/1, 2017.
[32] F. Inanlou, E. Kenyon, and J. Cressler, "An investigation of total ionizing dose damage on a pulse generator intended for space-based impulse radio UWB transceivers," *IEEE Trans. Nucl. Sci.*, vol. 60, no. 4, pp. 2605–2610, Aug. 2013.
[33] D. C. Howard *et al.*, "An 8–16 GHz SiGe low noise amplifier with performance tuning capability for mitigation of radiation-induced performance loss," *IEEE Trans. Nucl. Sci.*, vol. 59, no. 6, pp. 2837–2846, Dec. 2012.
[34] U. Dorda *et al.*, "Status of the MedAustron ion beam therapy centre," in *Proc. 1st Int. Part. Accel. Conf.*, 2012, pp. 4077–4079.
[35] M. Kanazawa *et al.*, "RF cavity with co-based amorphous core," in *Proc. EPAC*, vol. 2006, pp. 983–985.